requires that the *cis*-$Mg(P_i)_2$ complex is an internal intermediate and as such it would not have direct access to solvent. Thus, the bis(phosphate) complex generated from an inert coordination complex of pyrophosphate should remain trapped in the active site of pyrophosphatase. This type of phenomenon is in fact observed with hexokinase-catalyzed reaction of glucose with bidentate CrATP wherein the bridged complex, $Cr(H_2O)_4$(glucose-6-P)(ADP), is trapped in the active site as a dead-end intermediate (Dunaway-Mariano & Cleland, 1980). As a result, one observes only single turnovers of CrATP by hexokinase. In contrast, the reaction rate of the pyrophosphatase-catalyzed hydrolysis of $Co(NH_3)_4PP$ as well as of $Cr(H_2O)_4PP$ (Knight et al., 1981) does not appear severely restricted by the rate of bis(phosphate) complex release, and therefore this complex must have access to the solvent. Therefore, pathway b of Scheme II appears to be most consistent with the data at hand. According to this pathway, the $Mg(H_2O)_4(P_i)_2$ is hydrolyzed directly to monodentate $Mg(H_2O)_5P_i$ which is subsequently released from the active site.

Supplementary Material Available

A table giving anisotropic thermal parameters for nonhydrogen atoms in the crystal structure, a list of all observed and calculated structure factors, and a stereo packing diagram of the crystal structure (13 pages). Ordering information is given on any current masthead page.

References

Anderson, B., Milburn, R. M., Harrowfield, J. M., Robertson, G. B., & Sargeson, A. M. (1977) *J. Am. Chem. Soc. 99*, 2652–2661.

Avaeva, S. M., Bakuleva, N. P., Baratwva, C. A., Nazarova, T. I., & Fink, N. Y. (1977) *Biochim. Biophys. Acta 482*, 173–184.

Cooperman, B. S., Panackal, A., Springs, B., & Hamm, D. J. (1981) *Biochemistry 20*, 6051–6060.

Cornelius, R. D., Hart, P. A., & Cleland, W. W. (1977) *Inorg. Chem. 16*, 2799–2805.

Cromer, D. T., & Waber, J. T. (1965) *Acta Crystallogr. 18*, 104–109.

Dunaway-Mariano, D., & Cleland, W. W. (1980) *Biochemistry 19*, 1506–1515.

Farrell, F. J., Kjellstrom, W., & Spiro, T. G. (1969) *Science (Washington, D.C.) 164*, 320–321.

Frey, C. M., & Stuehr, J. (1972) *J. Am. Chem. Soc. 94*, 8898–8904.

Hamm, D. J., & Cooperman, B. S. (1978) *Biochemistry 17*, 4033–4040.

Huang, S. L., & Tsai, M.-D. (1982) *Biochemistry 21*, 951–959.

International Tables for X-ray Crystallography (1974) Vol. IV, pp 148–151, Kynoch Press, Birmingham, England.

Jencks, W. P. (1980) *Adv. Enzymol. Relat. Areas Mol. Biol. 51*, 75–106.

Johnson, C. K. (1976) *ORTEP-II*, Report ORNL-5138, Oak Ridge National Laboratory, Oak Ridge, TN.

Knight, W. B., Fitts, S. W., & Dunaway-Mariano, D. (1981) *Biochemistry 20*, 4079–4086.

Konsowitz, D. M., & Cooperman, B. S. (1976) *J. Am. Chem. Soc. 98*, 1993–1995.

Lincoln, S. F., & Stranks, D. R. (1968) *Aust. J. Chem. 21*, 27–81.

Merritt, E. A., & Sundaralingam, M. (1980) *Acta Crystallogr., Sect. B B36*, 2576–2584.

Rapoport, T. A., Hohne, W. E., Heitman, P., & Rapoport, S. (1973) *Eur. J. Biochem. 33*, 341–347.

Smith, R. M., & Martell, A. E. (1976) *Critical Stability Constants*, Vol. 4, p 56, Plenum Press, New York.

Sperow, J. W., & Butler, L. G. (1976) *J. Biol. Chem. 251*, 2611–2612.

Springs, B., Welsh, K. M., & Cooperman, P. S. (1981) *Biochemistry 20*, 6384–6391.

Stewart, R. F., Davidson, E. R., & Simpson, W. T. (1965) *J. Chem. Phys. 42*, 3175–3187.

Tsai, M.-D., Huang, S. L., Kozlowski, J. J., & Chang, C. C. (1980) *Biochemistry 19*, 3531–3536.

Three-Dimensional Structure of the Complex of the *Rhizopus chinensis* Carboxyl Proteinase and Pepstatin at 2.5-Å Resolution†

R. Bott,* E. Subramanian, and D. R. Davies

ABSTRACT: An X-ray diffraction analysis has been carried out at 2.5-Å resolution of the three-dimensional structure of the *Rhizopus chinensis* carboxyl proteinase complexed with pepstatin. The resulting model of the complex supports the hypothesis [Marciniszyn, J., Hartsuck, J. A., & Tang, J. (1976) *J. Biol. Chem. 251*, 7088–7094] that statine (3-hydroxy-4-amino-6-methylheptanoic acid) approaches an analogue of the transition state for catalysis. The way in which pepstatin binds to the enzyme can be extended to provide a model of substrate binding and a model of the transition-state complex. This in turn has led to a proposed mechanism of action based on general acid–base catalysis with no covalent intermediates. These predictions are in general agreement with kinetic studies using several carboxyl proteinases, which together with their sequence homology and their common three-dimensional structures suggest that this mechanism can be extrapolated to all carboxyl proteinases.

No consensus exists on the mechanism of action of the carboxyl proteinases, despite the fact that they have been widely studied (Fruton, 1976; Tang, 1979; James, 1981; Clement, 1973; Silver & James, 1980; Antonov, 1978). This class of proteinase includes the mammalian enzymes pepsin, chymosin, renin, and cathepsin D, as well as a variety of fungal enzymes. All the carboxyl proteinases hitherto examined appear to be highly conserved in that they all have two active

† From the Laboratory of Molecular Biology, National Institute of Arthritis, Diabetes, and Digestive and Kidney Diseases, National Institutes of Health, Bethesda, Maryland 20205. *Received July 20, 1982.*

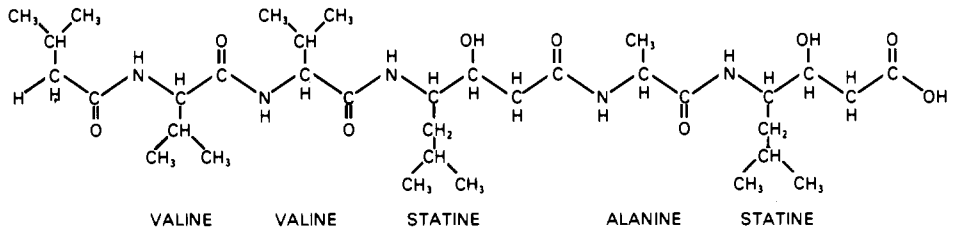

PEPSTATIN

FIGURE 1: Structure of pepstatin from *Actinomycetes* as determined by Umezawa et al. (1970).

aspartyl residues, a common molecular weight of approximately 35 000, a common specificity for peptide bonds located between large hydrophobic residues, and are inhibited by a common group of compounds (Tang, 1971; Fry et al., 1968; Takahashi & Chang, 1976). All carboxyl proteinase sequences are homologous in regions comprising approximately one-third of the molecule (Foltmann & Pedersen, 1977). The three-dimensional structures of four carboxyl proteinases have been reported and have been demonstrated to be very similar (Subramanian et al., 1977; Andreeva et al., 1978; Hsu et al., 1977).

We have determined the three-dimensional structure of a carboxyl proteinase from *Rhizopus chinensis* at 2.5-Å resolution (R. R. Bott, E. Subramanian, M. Liu, G. H. Cohen, W. A. Hendrickson, and D. R. Davies, unpublished experiments). The crystals of this enzyme have a particularly advantageous packing in which the active site is freely accessible to the inhibitors, such as the universal carboxyl proteinase inhibitor pepstatin (Figure 1), a hexapeptide isolated from strains of streptomyces (Umezawa et al., 1970). Pepstatin is an unusually potent inhibitor of carboxyl proteinases with a reported K_i for porcine pepsin of 4.5×10^{-11} M (Workman & Burkitt, 1979).

Pepstatin contains the unusual amino acid statine (3-hydroxy-4-amino-6-methylheptanoic acid), and it has been proposed that this statyl residue is responsible for the unusual inhibitory capability of pepstatin and that it is an analogue of the transition state for catalysis by the carboxyl proteinases (Marciniszyn et al., 1976). A low resolution (3.7-Å) analysis of pepstatin binding has been given previously (Subramanian et al., 1977b). In this paper we report the results of our analysis by X-ray diffraction of the three-dimensional structure of the pepstatin–*R. chinensis* proteinase complex at 2.5 Å. We discuss these results in terms of substrate binding and present a mechanism for the action of the enzyme.

Materials and Methods

The carboxyl proteinase from *R. chinensis* was obtained from Miles Laboratories. Pepstatin A was obtained from Sigma Chemical Co. Crystals of the proteinase were grown in the cold from a filtered 10 mg/mL solution of enzyme in 50 mM cacodylate buffer (pH 6.0)–20 mM calcium acetate. The crystals have the space group $P2_12_12_1$, with $a = 60.33$ Å, $b = 60.66$ Å, and $c = 107.0$ Å. Crystals of the enzyme–pepstatin complex were prepared in two ways: (1) by soaking crystals of the enzyme in a solution of pepstatin dissolved in 10% methanol and cacodylate buffer; (2) by direct crystallization of the complex from a solution containing enzyme and pepstatin. The presence of bound pepstatin in the crystals was indicated by changes that had occurred in an *h0l* precession X-ray photograph compared wtih the corresponding photograph from a native crystal.

X-ray diffraction data for the native and inhibited crystals were collected on a Picker FACS-I automated diffractometer by using an ω step scan. Radiation decay was monitored by the deterioration of three standard reflections. In all cases the decay was linear and isotropic and never exceeded a 15% drop from the initial intensity. The data were corrected for Lorentz polarization effects and for absorption by using a semiempirical method (North et al., 1968). Four soaked crystals were used to collect data to 2.5 Å and the data sets were averaged together, giving an R factor ($\sum||\bar{F}| - |F_i||/\sum|\bar{F}|$) of 0.059 for 9000 reflections. Two inhibited crystals obtained by cocrystallization were used to collect an independent set of data to 2.5 Å and the data sets were merged together, giving an R factor of 0.03.

Difference electron density maps were prepared by using $|F_{pepstatin}| - |F_{native}|$ as amplitudes and calculated phases based on the refined native molecule at 2.5-Å resolution ($R = 0.265$). The map was contoured at levels of 2σ estimated from the algorithm $\sigma = 1/V^2\sum(|F_p| - |F_o|)^2$. A model of pepstatin bound to the enzyme was obtained by fitting a skeletal model of pepstatin to the difference electron density map by using BILDER, an interactive graphics program written for the Evans & Sutherland Picture system by Dr. R. Diamond and implemented at the National Institutes of Health by Dr. G. Cohen. This fitting required a standard group for 3-hydroxy-4-amino-6-methylheptanoic acid which was based on the coordinates of the crystal structure of the *N*-(*p*-bromobenzoyl) derivative of 3-hydroxy-4-amino-6-methylheptanoic acid (Nakamura et al., 1973).

Results

Crystals of the enzyme–pepstatin complex prepared by soaking pregrown crystals in pepstatin and also by cocrystallization were isomorphous within the error of measurement. The R factor between native and inhibited data, $\sum||F_o| - |F_p||/\sum|F_o|$, was 0.145 for the soaked crystals and 0.16 for the crystals prepared by cocrystallization. The corresponding R factor between the 8340 reflections common to the two inhibited data sets was 0.10. The binding of pepstatin to the enzyme can be readily visualized in the difference electron density map. Maps calculated with data from inhibited crystals prepared by either soaking or cocrystallization were virtually identical. The principal feature of both maps is a continuous length of density that was taken to represent the pepstatin molecule (Figure 2). The remainder of the difference map is almost featureless, suggesting that the pepstatin binding does not drastically perturb the native conformation of the enzyme.

A skeletal model of pepstatin could easily be fitted to the density in the form of an extended chain. The chain direction was deduced from the size and shape of the side chain densities. Pepstatin is an asymmetric molecule (Figure 1) in which the N-terminal half has three valyl side chains while the C-terminal half contains the residues statylalanylstatine. One end of the continuous density could be fitted well with the sequence isovalerylvalylvalylstatine, thus determining the chain direction (Figure 2). The remainder of the density is more ambiguous, with the orientation of the Cβ of alanine-5 unresolved and with

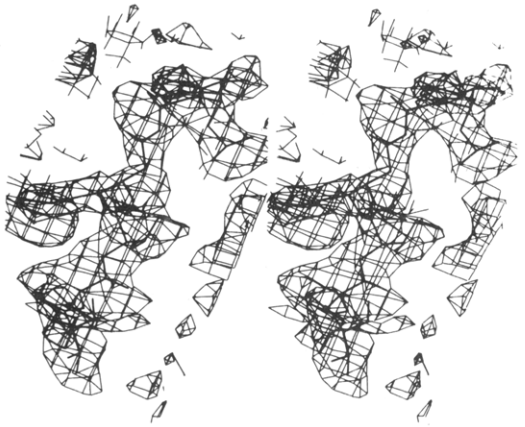

FIGURE 2: Model of pepstatin fitted to the difference electron density map, $|F_o| - |F_c|\alpha_{calcd}$, at 2.5-Å resolution. The isovaleryl group is at bottom with the statine-6 residue on top. Note the abrupt change in direction following the 3-OH of statine-4.

some ambiguity in the conformation of statine-6, perhaps because of disorder. The presence of statine-4 introduces two additional backbond atoms as compared with a normal polypeptide and prevents the residues alanine-5 and statine-6 from binding in the manner of a polypeptide substrate.

The model of pepstatin was derived solely from an interpretation of the difference electron density map without reference to the protein structure. Nevertheless, the resulting model makes reasonable contacts with the enzyme. Pepstatin is bound in the cleft, with the leucine-like side chain of statine-4 in a hydrophobic pocket formed by residues Tyr-79, Gly-80, Leu-81, Phe-117, and Leu-124, while the 3-hydroxyl oxygen of this statine residue straddles the carboxyls of the two active aspartyl residues at positions 35 and 220, and the amide N forms a hydrogen bond with the carbonyl of Gly-222. The remainder of the pepstatin also makes favorable interactions (Figure 3) with the protein. The carbonyl oxygen of Ala-5 hydrogen bonds to the Tyr-196 OH. The side chains of valine-2, valine-3, and statine-6 interact with hydrophobic residues which line the cleft. In particular, the side chain of statine-6 is bound to a pocket formed by Tyr-196, Ile-218, and Ile-300.

As noted above, the remainder of the difference electron density map is almost featureless. The main exception is in the vicinity of a β-hairpin loop containing residues 75–85, the "flap". We have interpreted this feature to indicate movement of the tip of the flap down onto the side chain of statine-4. The rest of the protein does not appear to undergo any noticeable conformational change when pepstatin is bound.

Discussion

The X-ray results presented above lead to a model in which pepstatin is bound deep in the cleft of the enzyme, with statine-4 at the catalytic site. Examination of this model indicates that in order to provide accessibility of the cleft to pepstatin, some movement of the flap relative to the protein must occur. Since what we observe crystallographically are the two end states, we cannot be sure that other changes do not also occur during the process of pepstatin binding, but the simplest model would involve some opening of the flap, followed by binding of pepstatin and subsequent closing of the flap. The difference electron density map does show some small movement of the flap relative to the unbound state. This movement may play a role in forming an adjustable hydrophobic pocket, providing an example of induced fit where the site can be finely tuned to the particular substrate side chain which would be leucine, phenylalanine, tyrosine, or tryptophan.

The quality of the pepstatin difference electron denstiy map in the region of statine-4 suggests that this portion of pepstatin is rigidly bound. The enzyme makes quite specific interactions with the enantiomorph of statine-4 present in pepstatin, namely, 3*S*,4*S* (Kinoshita et al., 1973), in agreement with studies which demonstrate that this enantiomorph is the most effective inhibitor of pepsin (Liu et al., 1979; Rich et al., 1977, 1980). Changing the hand of the side chain from 4*S* to 4*R* (L- to D-amino acid) increases the K_i by 100–10000 depending on the substrate (Liu et al., 1979). Changing the hand of the hydroxyl from 3*S* to 3*R* (Rich et al., 1980) or removing the 3-hydroxyl group (Rich et al., 1977) increased the K_i by a factor of 3000 and 2000, respectively. Our observation of tight binding (Figure 3) is consistent with these solution studies on the interaction of pepstatin with pepsin.

Comparative kinetic studies with synthetic substrates on both the *R. chinensis* enzyme and pepsin suggest that several residues on either side of the scissile bond influence the rate of catalysis (Voynick & Fruton, 1971; Sampath-Kumar & Fruton, 1974). These studies have shown that four residues on the amino side and at least three on the carboxyl side enhance the rate of catalysis. Hofmann and co-workers (Wang & Hofmann, 1976a) have shown from transpeptidation studies that pepsin is capable of binding an octa- or nonapeptide and that the binding is facilitated by medium-sized hydrophobic residues such as leucine and methionine. The *R. chinensis* enzyme shows a pattern of k_{cat}/K_m for a series of synthetic substrates roughly similar to that observed for pepsin (Voynick & Fruton, 1971; Sampath-Kumar & Fruton, 1974). Both enzymes have an identical sequence around the two active carboxyl acids labeled by 1,2-epoxy-3-(nitrophenoxy)propane and diazo-DL-norleucine methyl ester (Nakamura & Takahashi, 1978). Accordingly we have made use of the extensive kinetic data on pepsin in what follows, where we employ model building to interpret the binding of pepstatin with regard to substrate binding and the mechanism of action of the *R. chinensis* enzyme.

Model Building. (*1*) *Substrate.* The manner in which pepstatin binds to the enzyme leads naturally to a model in which the substrate binds as an extended chain. We use the convention of Berger & Schechter (1970) to designate enzyme

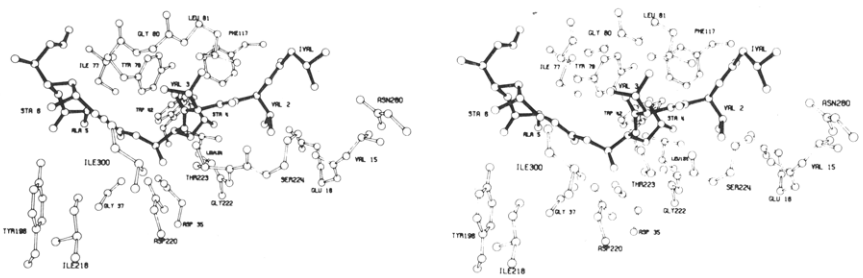

FIGURE 3: Rhizopus pepsin active site with pepstatin. Pepstatin (solid bands) binds in the cleft with the statine-4 side chain bound in a hydrophobic pocket formed by residues 79–80 of the flap and residues 117 and 124, while the 3-OH straddles the carboxyl moieties of the two active aspartic acids residues 35 and 220.

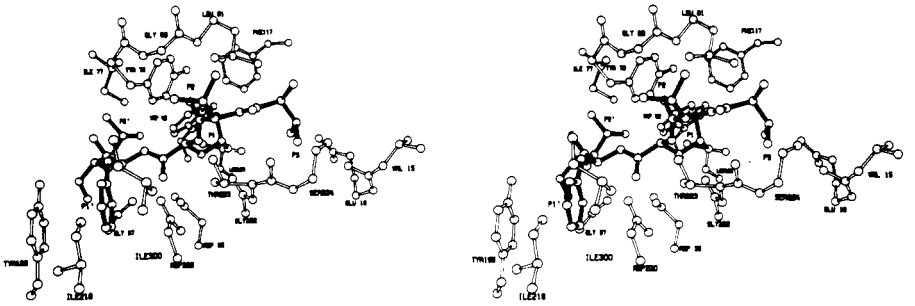

FIGURE 4: Model of a hypothetical substrate Val-Val-Leu-Phe-Leu (solid bands) in the active site of rhizopus pepsin. The first three residues were thethered to the corresponding residues in the model of pepstatin. The final two residues were built as an extended chain. The putative enzyme subsites for bind substrate are labeled by using the convention of Berger & Schechter (1970).

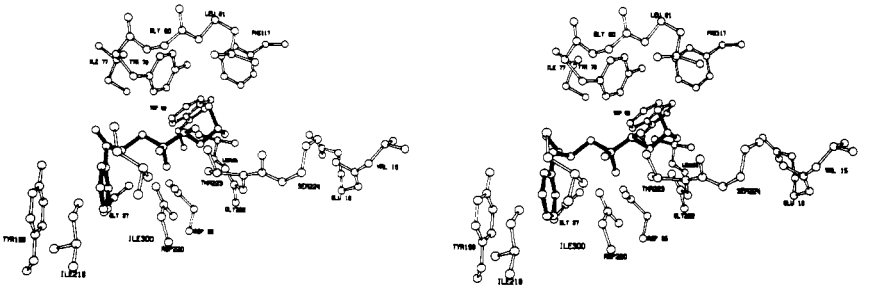

FIGURE 5: Model of a hypothetical tetrahedral intermediate based on the model of pepstatin (Figure 3) and modeled substrate (Figure 4). The model was constrained to keep the side chains bound at the putative subsites P_1 and $P_{1'}$ fixed.

subsites (P_3, P_2, P_1, $P_{1'}$, $P_{2'}$, $P_{3'}$, etc.), where the catalytic site is located between subsites P_1 and $P_{1'}$. The N-terminal isovaleryl group of the pepstatin is bound at P_4, valine-2 at P_3, valine-3 at P_2 and statine-4 is bound at P_1. Our substrate binding model would, of course, use the same protein subsites. We constructed a hypothetical substrate (Val-Val-Leu-Phe-Leu) as follows: the first two valines were superimposed on valines-2 and -3 of pepstatin, and the amino nitrogen, α carbon and side chain of the first leucine were superimposed on the corresponding atoms of statine-4. The remaining residues were oriented in an extended chain conformation and differed considerably from the remainder of pepstatin. The substrate built in this manner could be accommodated in the active site without any rearrangement of the enzyme. The phenylalanine side chain makes a very reasonable interaction with a hydrophobic pocket formed by residues Tyr-196, Ile-218, and Ile-300, with stacking of the aromatic side chains of the phenylalanine and Tyr-196 and with van der Waals contacts between the side chain of phenylalanine with Ile-218 and Ile-300. In this model of the substrate the carbonyl oxygen of the scissile peptide bond is directed toward the carboxyl oxygen of Asp-220 and away from the carboxyl oxygen of Asp-35. This is compatible with the expectation that at the active pH, Asp-220 is protonated while Asp-35 is deprotonated. An additional residue can be accommodated in the active site by continuing the extended polypeptide chain with hydrophobic side chains interacting with alternate sides of the cleft (Figure 4).

In view of the fact that these studies with the *R chinensis* proteinase crystals were conducted at pH 6, outside the pH range of optimum activity (pH 3–5), it is reasonable to ask whether the structure of the active site differs significantly from the active form. No structural data exist at present for this enzyme at pH 4 although we have observed that our crystals appear to tolerate this without extensive cracking. We have compared the three-dimensional structure of this proteinase with the only other carboxyl proteinase structure available at comparable resolution, penicillopepsin, which was crystallized at pH 4.4 (Hsu et al., 1977). The active sites of these enzymes are remarkably similar (R. R. Bott, E. Subramanian, M. Liu, G. H. Cohen, W. A. Hendrickson, and D. R. Davies, unpublished experiments). We have examined how our modeled substrate would interact with the active site of penicillopepsin and find that the pentapeptide substrate can easily be accommodated as an extended chain without rearrangement of either the substrate or the enzyme. At P_1 and $P_{1'}$ we find nearly identical enzyme–substrate interactions in both carboxyl proteinases. Corresponding residues in the two enzymes are highly conserved and can be superimposed. Interestingly, the P_1 residues Phe-117 and Leu-124 of the *R. chinensis* enzyme correspond to residues Phe-111 and Leu-120 of penicillopepsin which are separated by eight residues instead of six and yet both pairs form nearly identical van der Waals contacts with the leucine side chain at S_1.

The key residues predicted from the model to be involved with substrate binding at P_1 and $P_{1'}$ appear to be conserved in all sequenced carboxyl proteinases, and thus it is likely this mode of substrate binding will be relevant to the whole class of carboxyl proteinases.

(*2*) *Tetrahedral Intermediate.* Marciniszyn et al. (1976) suggested that statine-4 could be an analogue of the transition state for catalysis by the carboxyl proteinases. The observed binding of pepstatin places the hydroxyl group on the tetrahedral C3 atom of statine-4 in direct contact with the two aspartate carboxylates, with its side chain bound in a well-defined hydrophobic pocket. While the details of the observed binding differ from that proposed by Marciniszyn et al., the observed model does support their suggestion that the unusual inhibitory capacity of pepstatin could be the result of statine-4 approaching a transition-state analogue.

Accordingly, we have attempted to model the tetrahedral intermediate using the model of the substrate as a starting point. A plausible model may be constructed by adding a second OH in place of the hydrogen at C3 of statine-4. This hydroxyl makes no bad contacts with the *R. chinensis* proteinase active site and is in contact with the carboxyl oxygen OD1 of Asp-35 and with the carbonyl oxygen of Gly-37 (Figure 5). The model also includes a phenylalanine side

Table I: Comparison of Intermolecular Contacts (within 4 Å) between the Model of a Tetrahedral Intermediate [CA-C(OH)$_2$-N] in the Active Sites of the *R. chinensis* Carboxyl Proteinase and Penicillopepsin [Determined at pH 4.4 by Hsu et al. (1977)]

tetrahedral intermediate, atom	rhizopus pepsin		penicillopepsin[a]	
	atom	distance[b] (Å)	atom	distance[b] (Å)
CA	Asp-35 OD1	3.8	Asp-32 OD1	3.0
CA			Asp-32 CG	3.6
CA			Asp-32 OD2	3.7
CA	Gly-222 O		Gly-217 O	3.4
C	Asp-35 OD1	3.1	Asp-32 OD1	2.5
C			Asp-32 OD2	3.2
C			Asp-32 CG	3.2
C	Gly-37 O	3.7		
C			Asp-215 OD1	3.8
C	Asp-220 OD2	3.5	Asp-215 OD2	3.8
O1	Asp-35 OD1	3.9	Asp-32 OD1	3.6
O1			Asp-32 OD2	3.6
O1			Asp-215 OD1	3.2
O1	Asp-220 CG	3.5	Asp-215 CG	3.2
O1	Asp-220 OD2	2.5	Asp-215 OD2	2.6
O1	Gly-222 O	4.0	Gly-217 O	3.9
O1	Thr-223 OG1	3.5	Thr-218 OG1	3.6
O2	Asp-35 OD1	1.7	Asp-32 OD1	1.3
O2	Asp-35 CG	2.7	Asp-32 CG	1.8
O2	Asp-35 OD2	3.2	Asp-32 OD2	1.9
O2	Asp-35 CB	3.8	Asp-32 CB	3.3
O2			Gly-34 CA	3.8
O2			Ser-35 CG	4.0
O2	Gly-37 O	2.8		
O2	Asp-220 OD2	3.4	Asp-215 OD2	3.3
O2			Asp-215 CG	3.9
O2			Asp-215 OD1	3.9
O2	Gly-222 O	4.0	Gly-217 O	3.9
N	Gly-37 O	3.7		
N	Tyr-79 CB	4.0		

[a] Penicillopepsin was repositioned to obtain maximum overlap with the corresponding main chain atoms of the rhizopus pepsin. This superposition aligned 236 of a possible 323 α carbons with a root mean square deviation of 1.1 Å. [b] These distances are presented here for comparison. The atomic coordinates of both are being refined at higher resolution.

chain in position $S_{1'}$, which is bound to the hydrophobic pocket at $P_{1'}$.

In this model the position of the second hydroxyl should suggest the origin of the nucleophile that attacks the substrate. In the *R. chinensis* enzyme a hydroxide ion from a water molecule rather than the OD1 of Asp-35 would appear to be this nucleophile. A water molecule located here would be held by hydrogen bonds to the carboxyl of Asp-35, the carbonyl oxygen of Gly-37, and possibly the OG of Ser-38 on a suitable orientation for attack in the carbonyl carbon of the peptide bond. It is unlikely that an acyl enzyme intermediate could form through the OD1 of Asp-35 due to the large separation between this atom and the substrate carbonyl carbon.

We can place the model of pepstatin and of the tetrahedral intermediate at the corresponding position in penicillopepsin. The contacts made between the tetrahedral intermediate and the two enzymes are listed in Table I. Both interact in a very similar manner. The main difference is the distance between O2 of statine-4 and OD1 of Asp-35; in penicillopepsin the corresponding OD1 of Asp-32 is too close to O2, 1.3 Å, for a nonbonded contact. Examination of Asp-32 in penicillopepsin shows that the OD1 can readily be moved away from the O2 by a simple adjustment of the side chain dihedral angles χ_1 and χ_2 while still preserving the hydrogen bond betweeen OD2 of Asp-32 and OD2 of Asp-215, which corresponds to Asp-220 in the *R. chinensis* proteinase. On the other hand, it would appear to be impossible to move the OD1 closer to

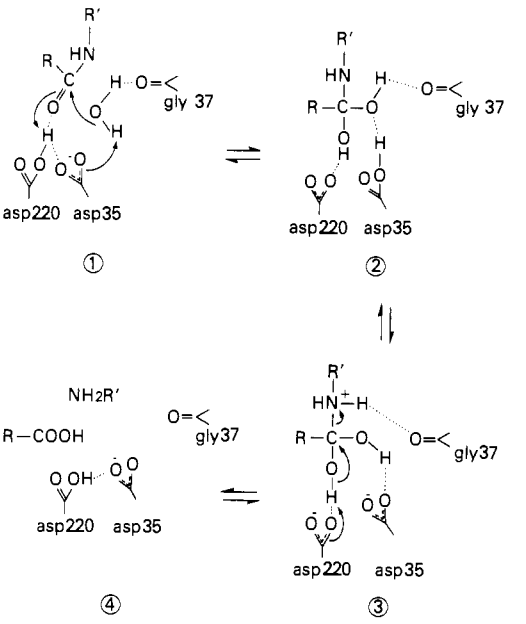

FIGURE 6: A diagrammatic representation of the mechanism of action based on the binding of pepstatin and model building of hypothetical substrate and tetrahedral complexes. The substrate binds with the peptide carboxyl directed toward the carboxyl of Asp-220 (215 in pepsin). The tetrahedral complex is formed by general acid–base catalysis with Asp-35 abstracting a proton from a bound water, and the hydroxide ion undergoes nucleophic attack at the carbonyl carbon, while Asp-220 polarizes the carbonyl bond. In step three, the carbonyl of Gly-37 could facilitate the shift of protons from the Asp-35 to the hydroxide and from the hydroxide to the amide nitrogen. This resulting complex breaks into products by elimination.

the peptide carbonyl without significant main chain movement so that a covalent intermediate also appears unlikely at pH 4. These results support the contention that the binding we observe and the modeling studies using the structure of the *R. chinensis* proteinase at pH 6 will be valid for the enzyme at pH 4.

(3) Mechanism. This model building study of the proposed tetrahedral intermediate leads naturally to a proposal for a mechanism for the carboxyl proteinases. We identify the hydroxyl oxygen of statine-4 with the carbonyl oxygen of our modeled substrate. This oxygen in the substrate is directed toward the protonated carboxyl of aspartic acid-220 (215 in pepsin). We postulate that, in the tetrahedral intermediate, it moves to a position roughly equidistant between the two carboxyl oxygens of Asp-35 (32 in pepsin) and Asp-220 where we find the hydroxyl of statine-4 of pepstatin. The second hydroxyl oxygen of the tetrahedral intermediate would come from the hydroxide ion of a water molecule. This water molecule could be ionized by interacting with the second carboxyl oxygen of Asp-35 and the carbonyl oxygen of Gly-37 (34 in pepsin).

We propose that the carboxyl of Asp-220 by base catalysis donates its proton to the carbonyl oxygen of the substrate while a water molecule loses a proton to Asp-35. This process may be concerted, in that the carboxyl of Asp-220 would form a hydrogen bond with Asp-35, so that when this proton is lost to the carbonyl oxygen of substrate, the carboxyl of Asp-35 becomes more electonegative and more capable of abstracting a proton from a water molecule and vice versa. The resulting hydroxide ion undergoes a nucleophilic attack on the carbonyl carbon of the substrate, giving the first tetrahedral intermediate (Figure 6).

This intermediate would be in equilibrium with a second intermediate in which the amide nitrogen is protonated. The

transfer of a proton to the amide nitrogen could be mediated by the carbonyl oxygen of Gly-37 which is within hydrogen bonding distance of the second hydroxyl oxygen and the amide nitrogen. The second tetrahedral intermediate is unstable and the products are created by a single elimination step. The mechanism we propose is a general acid–base catalysis with no covalent intermediate. This is a well-accepted mechanism for the hydrolysis of a peptide bond.

This mechanism shares several common features with the mechanism III proposed by James et al. (1980). In particular, both mechanisms propose nucleophilic attack by a hydroxide ion forming a noncovalent intermediate. However, the mechanism presented here involves base catalysis by Asp-35 and acid catalysis by Asp-220. In the James et al. mechanism, it is not clear how the water is activated since "Asp-32 is not assumed to activate the bound water because its p*K*a of ~ 1 is considerable lower than that of water". In our mechanism, we assume that the p*K* of Asp-32 (Asp-35 in *R. chinensis*) is raised as a result of the intrusion of the carbonyl of the substrate by a rearrangement of the Asp-32 side chain. The two mechanisms differ in the means of protonation of the amide nitrogen. In the James et al. mechanism, Tyr-79 OH is the electrophile, whereas in our mechanism a proton from the water serves as the electrophile via the carbonyl oxygen of Gly-37. Considerable movement of the Tyr-79 side chain is required in order to bring the hydroxyl into appropriate juxtaposition to the amide nitrogen, but in the pepstatin–proteinase complex we see no indication of such a motion; in fact this tyrosine forms part of the hydrophobic pocket at P_1 which should help stabilize its position. One additional difference with the James et al. mechanism concerns their proposal of an extensive charge relay network. We do not see, in the *R. chinensis* proteinase structure, the same arrangement of the necessary side chains to form this network.

In comparing these mechanisms, it should be kept in mind that they are both based on partially completed structures, in the case of penicillopepsin a 2.8-Å structure vs. a 2.5-Å structure of *R. chinensis* enzyme and the pepstatin–enzyme complex. It is certainly possible that a higher resolution analysis may result in changes that would affect either or both mechanisms.

The mechanism proposed here is in general consistent with a variety of chemical observations on carboxyl proteinases. With short peptide substrates, the carboxyl proteinases can catalyze transpepidation. In such a reaction larger peptides are formed via acyl or amino transfer and these are subsequently hydrolyzed to give peptide fragments not present in the original substrate (Wang & Hofmann, 1976a,b, 1977; Fruton et al., 1961; Takahashi et al., 1974; Newmark & Knowles, 1975). This has led to the assumption that catalysis by the carboxyl proteinases involves either a covalent acyl or an amino intermediate, in contrast to the mechanism proposed here which does not involve a covalent intermediate. Attempts to isolate the covalent intermediates have been unsuccessful (Cornish-Bowden et al., 1969). Newmark & Knowles (1975) have noted that transpeptidation need not involve a covalent intermediate and that the relative importance of acyl transfer or amino transfer may depend upon the ease with which the acyl and amino moieties of the cleaved substrate leave the active site.

Transpeptidation studies with [^{14}C]leucyltyrosyl[^{3}H]leucine (Newmark & Knowles, 1975) and leucyltyrosylmethionine (Wang & Hofmann, 1976a,b) indicate that for fragments, when either acyl or amino transfer occurs, the acyl transfer reaction predominates. The substrate binding we propose also suggests that the leucyl side chain of the acyl moiety would be more tightly bound at the P_1 site rather than the $P_{1'}$ site where a planar hydrophobic residue would be preferred. Consequently, leucine or methionine bound at the $P_{1'}$ site would have a greater ease of leaving the active site so that acyl transfer would predominate, as is in fact observed (Wang & Hofmann, 1976a; Newmark & Knowles, 1975). Substrate specificity studies using pepsin have also indicated a preference for planar hydrophobic residues of the $P_{1'}$ site (Powers et al., 1977).

Additional evidence favoring a noncovalent intermediate comes from studies of ^{18}O exchange during hydrolysis (Sharon et al., 1962) and transpeptidation (Antonov et al., 1978) in the presence of $H_2{}^{18}O$. It has been shown (Antonov et al., 1981) that ^{18}O is incorporated into nonhydrolyzed substrate. Antonov and co-workers postulate that this can only result from base catalysis to form a tetrahedral intermediate similar to the one we propose (step 2) and that the rate of decomposition of this intermediate to yield initial substrate is higher than that of its decomposition rate en route to the reaction product. This interpretation also necessitates that the two hydroxyl oxygens on the tetrahedral intermediate must be roughly equivalent so that in the reverse direction the substrate will contain ^{18}O. In our model the two hydroxyl oxygens are in similar environments. One hydroxyl oxygen interacts with the carboxyl oxygens of Asp-220 and Asp-35; the other hydroxyl oxygen interacts with the carboxyl of Asp-35 and the carbonyl of Gly-37. Therefore, in the reverse step, either hydroxyl could be released, giving the result reported by Antonov and co-workers.

The incorporation of ^{18}O from $H_2{}^{18}O$ into nonhydrolyzed substrate also suggests a rate-limiting step following the formation of the first tetrahedral intermediate. It is conceivable that the formation of the second tetrahedral intermediate (step 3) may be the rate-limiting step and in fact may involve a series of steps. This is, however, beyond the scope of the present study.

It has been postulated that the carboxyl proteinases undergo a conformational change during catalysis (Fruton, 1976; Wang & Hofmann, 1976b), which is not supported by our analysis of pepstatin binding. Evidence for this conformational change comes from kinetic studies using synthetic substrates in which increasing the substrate size by including residues such as glycine and alanine resulted in an increase in k_{cat} with little increase in K_m (Fruton, 1976), from circular dichroism (Wang & Hofmann, 1976b), and from the existence of activation peptides which are not cleaved but increase catalytic activity and transpeptidation (Wang & Hofmann, 1976b). An alternative explanation of these results is that increasing substrate length or adding an activation peptide may reduce the proportion of substrate involved in nonproductive binding. From transpeptidation studies, Hofmann and co-workers have shown that hydrophobic residues can bind at many subsites in the catalytic cleft so that short synthetic substrates could also bind to these sites nonproductively. If such binding has a similar affinity at different subsites, then blocking this binding would have little affect on K_m but may markedly increase k_{cat}, without a conformational change in the enzyme. With this interpretation in mind, the mechanism we propose is consistent with all the available kinetic data on the carboxyl proteinases.

The analysis of pepstatin binding has given us a better understanding of the interaction between substrate and enzyme. It has led to a model of the tetrahedral intermediate and a tentative mechanism of action. At present, we are

engaged in a higher resolution analysis of the X-ray structure with the expectation that a more precise model will provide further insight into the mechanism of action of these proteinases and into the design of additional inhibitors, both as potential therapeutic agents and as probes for the detailed study of the mechanism.

Added in Proof

A recent report using ^{13}C NMR (Rich et al., 1982) provides evidence for a tetrahedral intermediate in the binding of a pepstatin analogue to porcine pepsin. A crystallographic analysis of the binding of a fragment of pepstatin to penicillopepsin has also been reported (James et al., 1982).

Acknowledgments

We thank Drs. Ben Dunn, Theo Hofmann, and Daniel Rich for many helpful discussions and describing their results prior to publication, Drs. Louis Cohen and Jeremy Knowles for helpful discussions concerning the mechanism of action, and Drs. Gerson Cohen and Alexander Wlodawer for their critical reading of the manuscript.

References

Andreeva, N. S., Federov, A. A., Gutshina, A. E., Riskulov, R. R., Schutzkever, N. E., & Safro, M. G. (1978) *Mol. Biol. (Engl. Transl.) 12*, 922–935.

Antonov, V. K. (1978) *Proc. FEBS Meet. 51*, 95–103.

Antonov, V. K., Ginodman, L. M., Kapitannikov, Y. V., Barshevskaya, T. N., Gurova, A. G., & Rumsh, L. D. (1978) *FEBS Lett. 88*, 87–89.

Antonov, V. K., Ginodman, L. M., Rumsh, L. D. Kapitannikov, Y. V., Barshevskaya, T. N., Yavashev, L. P., Gurova, A. G., & Volkova, L. I. (1981) *Eur. J. Biochem. 117*, 195–200.

Berger, A., & Schechter, I. (1970) *Philos. Trans. R. Soc. London, Ser. B 257*, 249–264.

Clement, G. E. (1973) *Prog. Biorg. Chem. 2*, 177–238.

Cornish-Bowden, A. J., Greenwell, P., & Knowles, J. R. (1969) *Biochem. J. 113*, 369–375.

Foltmann, B., & Pedersen, V. B. (1977) in *Acid Proteinases, Structure, Function, and Biology* (Tang, J., Ed.) pp 3–22, Plenum Press, New York.

Fruton, J. S. (1976) *Adv. Enzymol. Relat. Areas Mol. Biol. 44*, 1–36.

Fruton, J. S., Fujii, S., & Knappenberger, M. H. (1961) *Proc. Natl. Acad. Sci. U.S.A. 47*, 759–761.

Fry, K. T., Kim, O.-K., Spona, J., & Hamilton, G. A. (1968) *Biochem. Biophys. Res. Commun. 30*, 489–495.

Hsu, I.-N., Delbaere, L. T. J., & James, M. N. G. (1977) *Nature (London) 266*, 140–145.

James, M. N. G. (1981) in *Structural Studies on Molecules of Biological Interest* (Dodgson, G., Clusker, G. P., & Sayre, D., Eds.) Clarendon Press, Oxford.

James, M. N. G., Sielecki, A., Salituro, F., Rich, D. H., & Hofmann, T. (1982) *Proc. Natl. Acad. Sci. U.S.A. 79*, 6137–6141.

Kinoshita, M., Aburaki, S., Hagiwara, A., & Imai, J. (1973) *J. Antibiot. 26*, 249–251.

Liu, W.-S., Smith, S. C., & Glover, G. I. (1979) *J. Med. Chem. 22*, 577–579.

Marciniszyn, J., Hartsuck, J. A., & Tang, J. (1976) *J. Biol. Chem. 251*, 7088–7094.

Nakamura, M., Morishima, H., Takita, T., Umezawa, H., & Iitaka, Y. (1973) *J. Antibiot. 26*, 255–256.

Nakamura, S., & Takahashi, K. (1978) *J. Biochem. (Tokyo) 84*, 1593–1600.

Newmark, A. K., & Knowles, J. R. (1975) *J. Am. Chem. Soc. 97*, 3557–3559.

North, A. C. T., Phillips, D. C., & Mathews, F. S. (1968) *Acta Crystallogr., Sect. A A24*, 351–359.

Powers, J. C., Harley, A. D., & Myers, D. V. (1977) in *Acid Proteases, Structure, Function and Biology* (Tang, J., Ed.) pp 141–157, Plenum Press, New York.

Rich, D. H., Bernatowicz, M. S., & Schmidt, P. G. (1982) *J. Am. Chem. Soc. 104*, 3535–3536.

Rich, D. M., Sun, E., & Singh, J. (1977) *Biochem. Biophys. Res. Commun. 74*, 762–767.

Rich, D. M., Sun, E. T. O., & Ulm, E. (1980) *J. Med. Chem. 23*, 27–33.

Sampath-Kumar, P. S., & Fruton, J. S. (1974) *Proc. Natl. Acad. Sci. U.S.A. 71*, 1070–1072.

Sharon, N., Grisaro, V., & Neumann, H. (1962) *Arch. Biochem. Biophys. 97*, 219–221.

Silver, M. S., & James, S. L. T. (1980) *J. Biol. Chem. 255*, 550–560.

Subramanian, E., Swan, I. D. A., Liu, M., Davies, D. R., Jenkins, J. A., Tickle, I. J., & Blundell, T. L. (1977a) *Proc. Natl. Acad. Sci. U.S.A. 74*, 556–559.

Subramanian, E., Liu, M., Swan, I. D. A., & Davies, D. R. (1977b) in *Acid Proteases, Structure, Function and Biology* (Tang, J., Ed.) pp 33–41, Plenum Press, New York.

Takahashi, K., & Chang, W.-J. (1976) *J. Biochem. (Tokyo) 80*, 497–506.

Takahashi, M. N., Wang, T.-L., & Hofmann (1974) *Biochem. Biophys. Res. Commun. 57*, 39–46.

Tang, J. (1971) *J. Biol. Chem. 246*, 4510–4517.

Tang, J. (1979) *Mol. Cell. Biochem. 26*, 93–109.

Umezawa, H., Aoyagi, T., Morishima, H., Matsuzaki, M., Hamada, M., & Takeuchi, T. (1970) *J. Antibiot. 23*, 259–262.

Voynick, F. M., & Fruton, J. S. (1971) *Proc. Natl. Acad. Sci. U.S.A.* 68, 257–259.

Wang, T.-T., & Hofmann, T. (1976a) *Biochem. J. 153*, 691–699.

Wang, T.-T., & Hofmann, T. (1976b) *Biochem. J. 153*, 701–712.

Wang, T.-T., & Hofmann, T. (1977) *Can. J. Biochem. 55*, 286–294.

Workman, R. J., & Burkitt, D. W. (1979) *Arch. Biochem. Biophys. 194*, 157–164.